

A SENSITIVITY ANALYSIS OF FACTORS AFFECTING THE WARPAGE OF A COMPOSITE STRUCTURE

Andrew Johnston¹, Pascal Hubert², Karl Nelson³, and Anoush Poursartip²

1-Institute for Aerospace Research, NRC, Ottawa, CANADA

2-Composites Group, Department of Metals and Materials Engineering,
The University of British Columbia, Vancouver, BC, CANADA

3-Boeing Defense & Space Group, Seattle, WA, USA

ABSTRACT

KEY WORDS: Composite Structures, Process Modelling, Warpage

1. INTRODUCTION

Modelling of materials processes is a well-established methodology. Over the past two decades, a number of increasingly capable computational models for the autoclave processing of thermoset matrix laminated composite materials and structures have been developed [e.g. 1-10]. Some of these models have focused largely on a single phenomenon such as heat transfer and resin reaction kinetics [e.g. 4,6,7], resin flow [e.g. 2], or stress development [e.g. 8,9] while others have been more broad in scope examining a number of important processing phenomena and their interactions [e.g. 1,3,5,10].

1.1. COMPRO Process Modelling Software

In this paper we use COMPRO, a two-dimensional finite element process modelling software developed by the Composites Group at The University of British Columbia specifically to analyse industrial autoclave processing of composite structures of intermediate size and complexity. COMPRO incorporates analyses of a number of important processing mechanisms including component internal temperature, resin degree of cure, resin flow and the development of residual stress and deformation. This software can examine complex 2-D structures with multiple composite and non-composite materials, including the effects of process tooling and autoclave characteristics. A more detailed description is given in [10].

A modular approach is employed for the overall program structure, similar to that described by Loos and Springer [1]. The main body of the program consists of a series of ‘modules’, each responsible for performing a single task such as calculating resin flow (the ‘flow-compaction’ module) or development of internal stresses (the ‘stress-deformation’ module). The various

modules are called as needed by a controlling routine as the solution marches forward in time. At the beginning of each time step, an ‘autoclave controller’ module, simulating automated autoclave control, updates all process variables including the autoclave air temperature, the autoclave pressure and the vacuum bag pressure. A central database containing a description of the modelled components (i.e. composite, tool, inserts, etc..) is updated by each solution module as it is called.

1.2. Aim of This Paper

The purpose of this paper is to show the results of a comprehensive sensitivity study of the effect of key analysis parameters, thermophysical and mechanical properties, and boundary and initial conditions on the predicted warpage of a realistic structure.

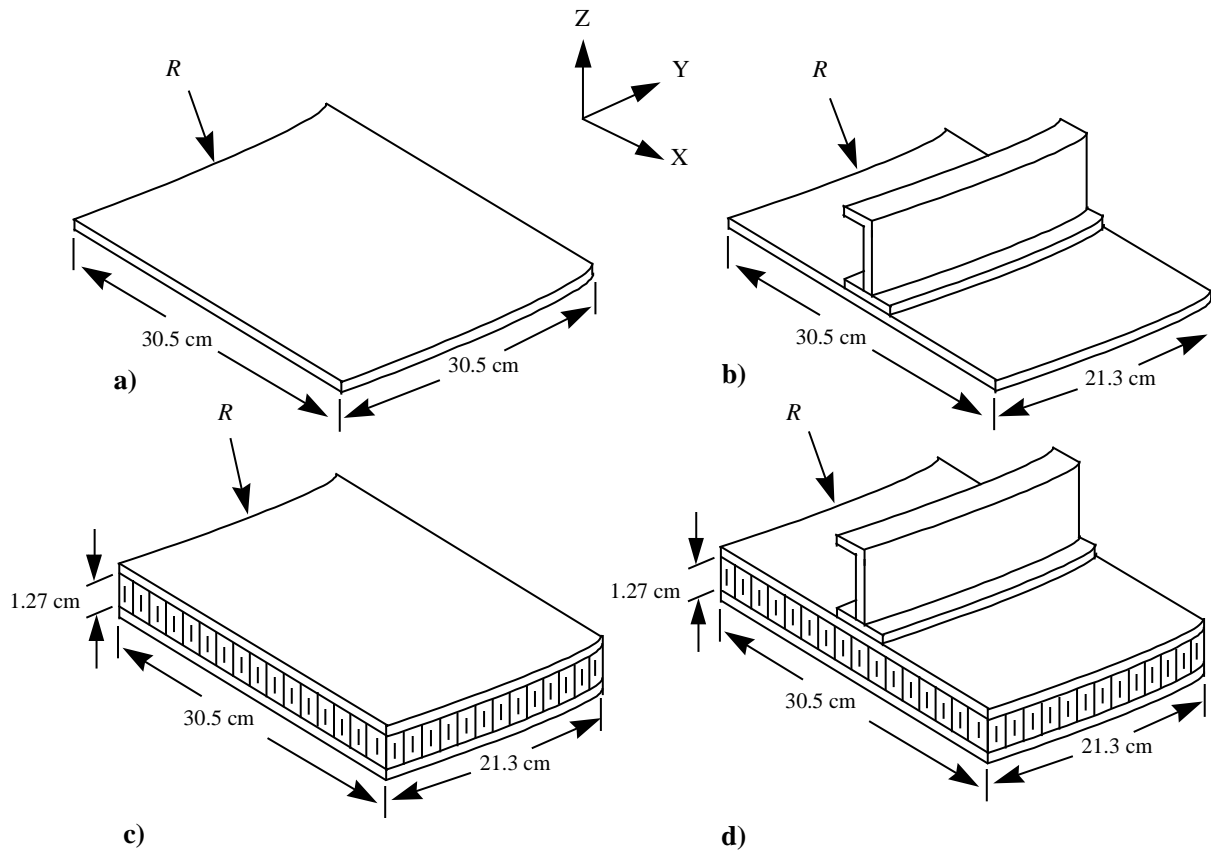
2. PREDICTIONS FOR A J-STIFFENED STRUCTURE

This paper builds on a previous analysis of a J-stiffened structure [11]. These structures are illustrated in Figure 1. The face sheets for both parts were made of 12-ply of Hercules AS4/8552 grade 190 prepreg tape with [45/90/-45/0/45/90]_s lay-up. A single pre-cured braided J-frame made by RTM was centred on the top face sheet and bonded to it using Cytec Metlbond 1515 structural adhesive, which is also used to bond the skins to the Hexcel HRP 0.1 kg/m³ (8 lb/ft³) honeycomb core. No special tooling was used to prevent the frames from shifting during cure. Finite element descriptions of all parts were generated for COMPRO using the PATRAN preprocessor. An example of the FE discretization is shown in Figure 2.

The parts were assembled on a large aluminum tool with a constant radius of curvature of 3.10 m (122”) in the y-direction and cured using the process cycle shown in the inset in Fig. 2. To examine part-to-part variability, three samples of both components were built. As a baseline, three samples of skins and honeycomb structures with no frames were also built.

Dividing the analysis into a series of four problems allows independent examination of warpage sources in the simpler structures where perhaps only one mechanism is dominant before tackling the most complex problem (the stiffened honeycomb structure), in which several competing mechanisms may be present.

The first of the substructures examined is the unstiffened skin. For this simple structure, the dominant source of deformation was found to be the tooling constraint. As discussed in [11], the level of tool/part interaction, modelled via the shear layer, is a significant unknown. This structure is ideal for examining tool/part interaction since this is the dominant deformation mechanism and the low thickness of the part (12 plies) and its large span (30 cm total) result in easily measured warpage.



Notes:

- $R = 3.10$ m (tool side)
- Core - Hexcel Glass/Phenolic HRP with 130 kg/m^3 (3/16" cell dia.)
- Face sheet layup $[45/90/-45/0/45/90]_s$
- Frames pre-cured and adhesively bonded to face sheets

Figure 1 Structures examined in this paper: a) unstiffened skin laminate, b) stiffened skin laminate, c) unstiffened honeycomb structure, d) stiffened honeycomb structure.

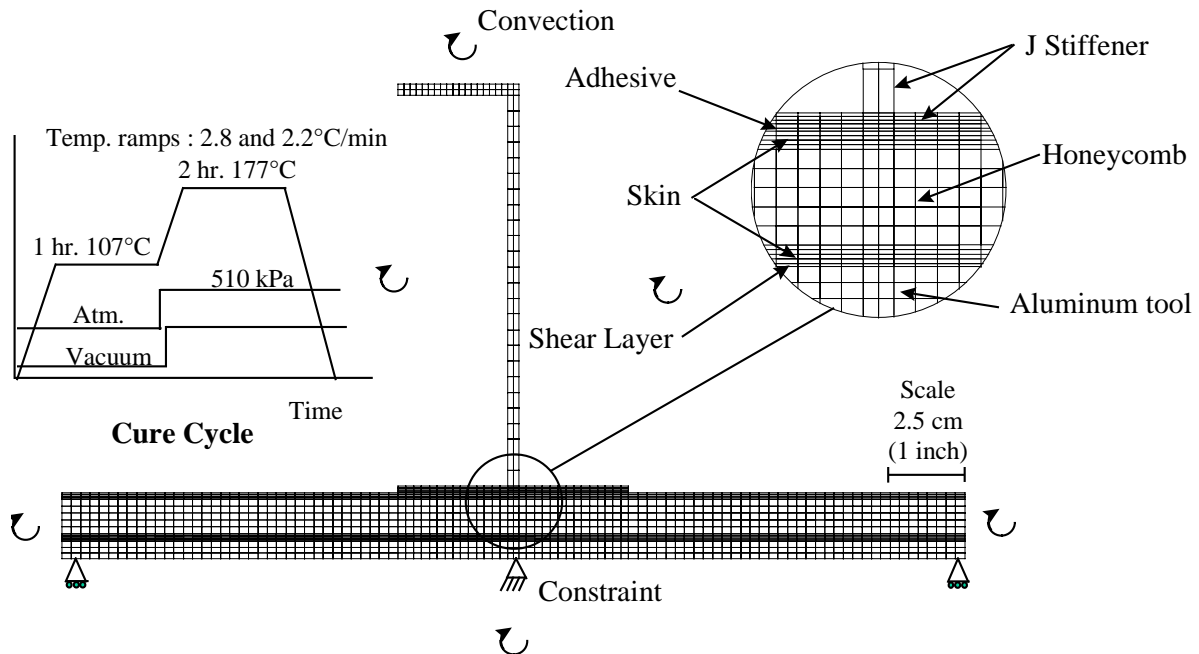


Figure 2 Finite Element Representation of Honeycomb and J-frame Structure

The effect of shear layer on the predicted unstiffened skin warpage was examined by varying its modulus over a wide range. Using a low shear layer modulus results in a nearly symmetric residual strain profile through the skin thickness and thus only a very low level of warpage.

The significant constraint of a high shear layer modulus, however, results in generation of an unsymmetric residual strain profile, and thus much higher warpage.

As shown in Figure 3, the maximum predicted deflection is found to be very highly dependent on shear layer modulus. Comparing predicted warpage to that actually measured, a shear layer shear modulus, G_{SL} , of 5×10^4 Pa has been chosen as the baseline. Figure 4 shows that this choice results in a very good fit to experimental measurements in both warpage shape and magnitude.

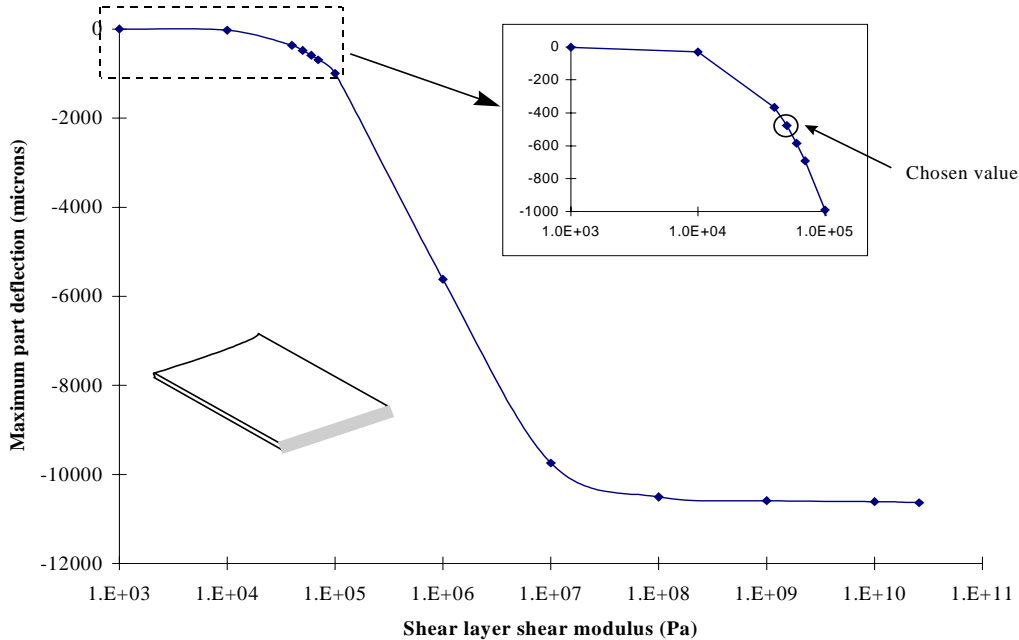


Figure 3. Shear layer calibration using unstiffened skin part.

Two major sources of process-induced deformation are apparent for the unstiffened honeycomb structure. One is tool/part interaction, the same as for the unstiffened skin. The other is the rather large lag between the temperatures of the top and bottom skins due to the large thermal mass of the tool and the low air/tool heat transfer rates in this case. As illustrated in Figure 5, this temperature gradient results in corresponding gradients in the cure rate of the two skins and consequently in differences in the rate of resin modulus development. The combination of these hardening gradients with the rapid change in thermal and cure shrinkage strains at this point in the process results in the development of residual stress.

Figure 6 shows a comparison between measured and predicted warpage for this structure. It is difficult to say how good the agreement is in this case because of the large amount of scatter in the experimental data and since two of the specimens warped predominantly upwards and one downwards. All that can truly be concluded is that the deformation is of the same order of magnitude as measured. Two sources of potential error in this prediction should be pointed out. One is the rather large uncertainty in the honeycomb moduli employed in the prediction. Also, the adhesive layer between the honeycomb and skins were not modelled. It is unclear how predictions would be affected by either of these factors.

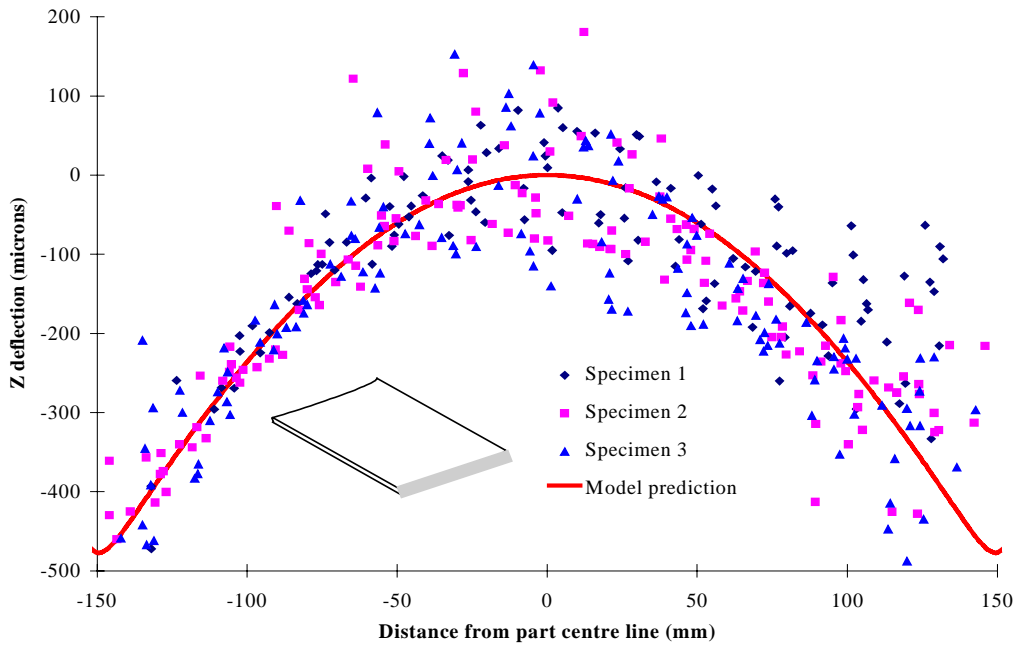


Figure 4. Warpage prediction for unstiffened skin with calibrated shear layer.

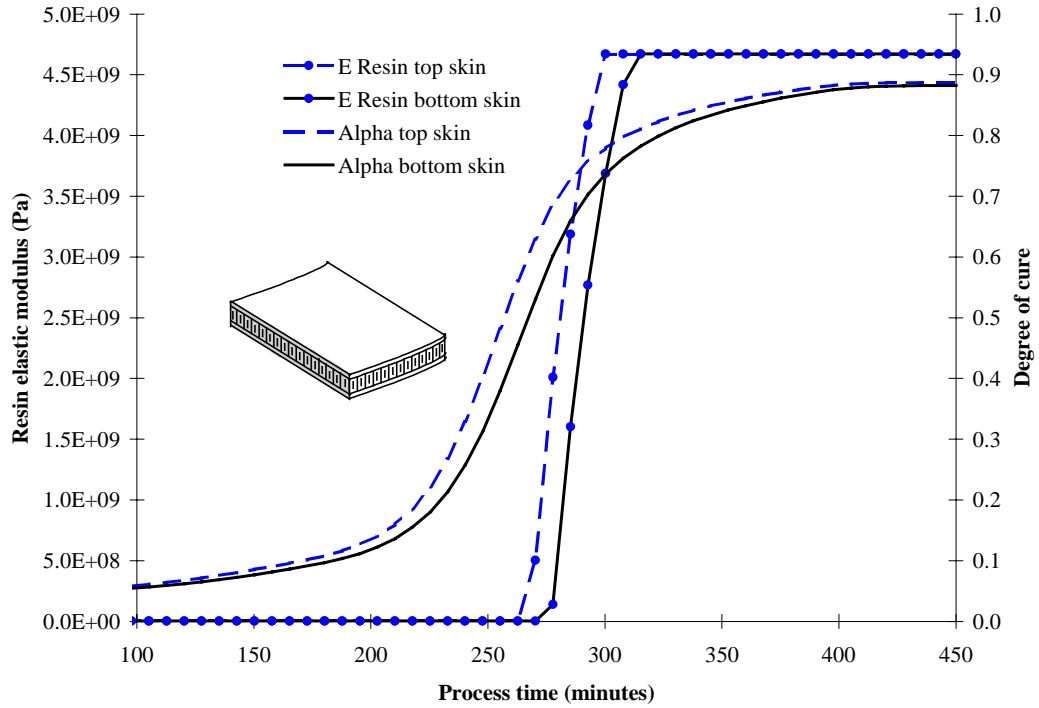


Figure 5. Predicted resin degree of cure and resin modulus in top and bottom skins of unstiffened honeycomb structure.

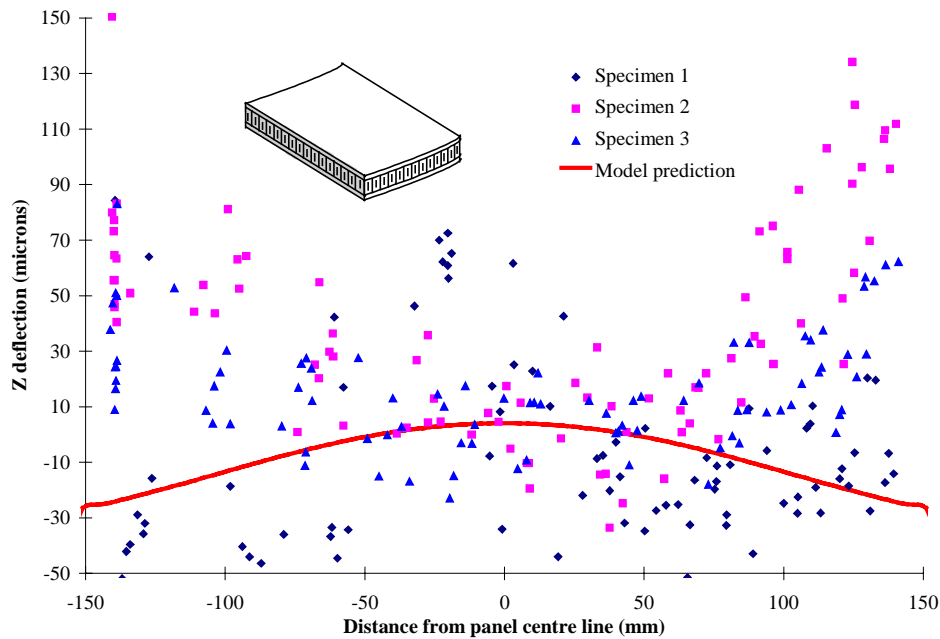


Figure 6. Model warpage prediction for unstiffened honeycomb panel.

The next part examined was the stiffened skin structure. For this structure, it was clear from the observed warpage pattern that the major source of warpage was an interaction between the skin and the J-frame. However, initial attempts to model this part resulted in very poor results, indicating warpage in the *opposite direction* to that actually measured. Closer examination of the problem revealed that an important factor had been overlooked. The J-frame includes on its underside an adhesive noodle that had not been included in the original model. Re-doing the analysis, this time incorporating a geometrically crude representation of this noodle, resulted in the predicted post-processing shape shown in Figure 7.

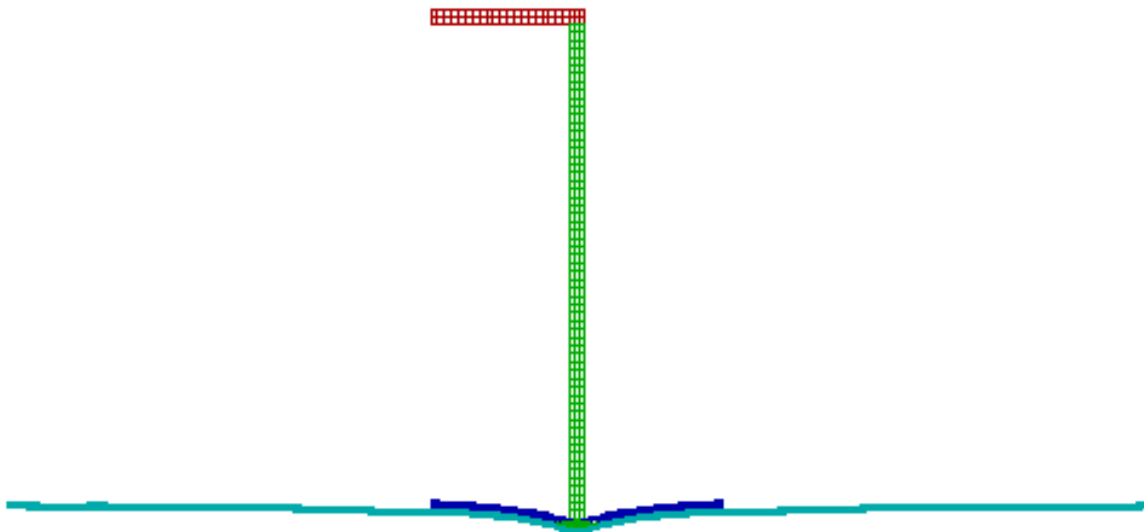


Figure 7. Predicted post-processing shape of J-stiffened skin part with modelling of adhesive noodle (displacements exaggerated by a factor of 10).

This magnitude of the predicted deflection from this new model agreed much better with experimental results. However, the bulk of the warpage was predicted to be much too localized, reflecting the crudity of the used geometric representation of the noodle. Unfortunately, model limitations on the number of elements prevented a more detailed geometric description of this region of the foot from being used. For this reason, the effect of the noodle was instead incorporated into the analysis by calibrating the *CTE* of the entire J-

frame foot such that good agreement was obtained with measured total part deflection. Figure 10 shows that neither this ‘distributed strain’ approach nor the crude noodle model accurately predict the shape of the warpage directly beneath the foot, but act as bounds to the actual shape. A more accurate model of the noodle structure would be expected to produce better fit in this region.

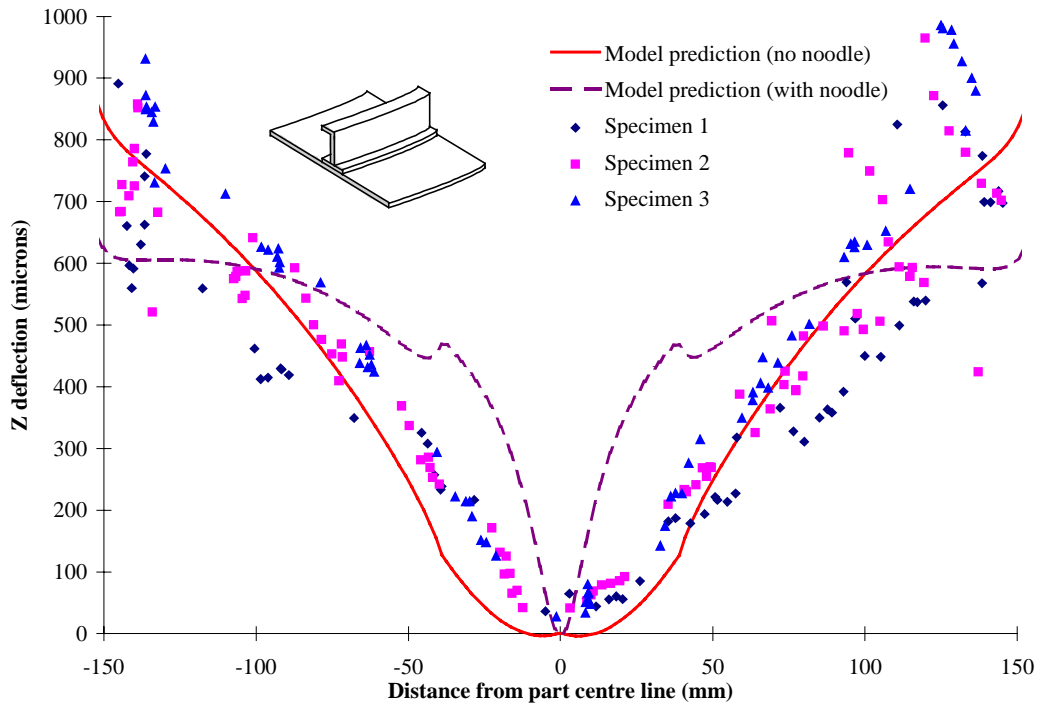


Figure 8. Model warpage prediction for J-stiffened skin structure showing best fit prediction and prediction with crude adhesive noodle model.

The final part examined, representing a synthesis of the other three, is the stiffened honeycomb structure. All of the deformation mechanisms acting in the other structures play a role in determining the final shape of this structure. Fortunately, since analyses of these deformation sources have already been performed in the simpler parts, modelling of this structure is quite straightforward. The predicted underside deformation for this case is compared to measurements in Figure 9. As shown in this figure, a somewhat lower maximum deflection is predicted than obtained from experiment (about 0.12 mm versus 0.15 mm). Away from the foot of the frame, the ‘slope’ of the predicted deformation is in quite good agreement to that measured, but warpage in the area directly beneath the foot is not well predicted. This points to the most likely source of the observed disagreement as being the distributed foot *CTE* representation of the adhesive noodle. However, as is discussed in the sensitivity analysis following, the predicted warpage in this case is quite sensitive to input parameters, and other factors may also be involved.

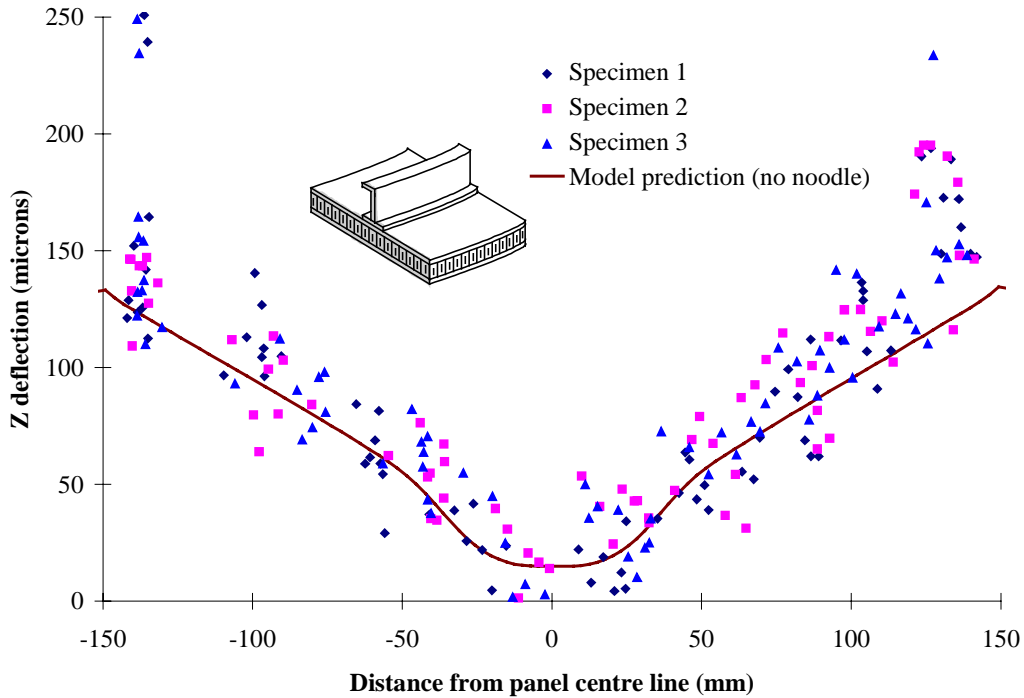


Figure 9. Model warpage prediction for J-stiffened honeycomb panel (nominal case).

2.1. Sensitivity Analysis

The focus of the sensitivity analysis is the effect of variability in process parameters on process-induced deformation. In this analysis the *maximum* underside deflection of the stiffened honeycomb structure is examined. The parameters examined in this sensitivity study are outlined in Table 1 including the ‘high’ and ‘low’ values employed in each case.

Sensitivity analysis predictions for a number of parameter categories are summarized graphically in Figures 10-12. Analysis parameters had little effect on predicted deflection, nor did any composite thermophysical properties with the exception of resin cure kinetics (Figure 10).

As shown in Figure 11, boundary and initial conditions (including tool material) were of intermediate importance, with all parameters except initial degree of cure having a significant influence on predicted warpage. Varying the mechanical properties of the various materials in the structure (Figure 12) had the greatest effect on deformation predictions. For the range of property values examined, predicted deflections ranged from -0.06 mm to 0.23 mm.

Table 1. Parameters examined in sensitivity analysis.

<i>Parameter</i>	<i>Nominal Value</i>	<i>High Value</i>	<i>Low Value</i>
<i>Analysis parameters</i>			
Maximum Overall Time Step (s)	30	100	10
Maximum Degree of Cure Step (Stress)	0.05	0.10	0.025
Maximum Percentage Change in E_{resin} (Stress)	10	20	5
<i>Thermophysical properties</i>			
Resin Specific heat capacity (J/kgK)	$1300 + 4.29 * T - 369 * \alpha$	$2790 - 3.80 * T^{(1)}$	$1005 - 369 * \alpha^{(2)}$
Resin Thermal conductivity (W/mK)	$0.148 + 3.43 \times 10^{-4} * T + 6.07 \times 10^{-2} * \alpha$	$0.185 + 4.293 \times 10^{-4} * T + 7.59 \times 10^{-2} * \alpha (+25\%)$	$0.155 + 6.07 \times 10^{-2} * \alpha^{(2)}$
Honeycomb	$0.0774 + 3.4 \times 10^{-4} * T$	$0.0968 + 4.25 \times 10^{-4} * T (+25\%)$	$0.0581 + 2.55 \times 10^{-3} * T (-25\%)$
Fibre V_f (-)	0.573	0.602 (+5%)	0.544 (-5%)
Resin heat of reaction (J/kg)	540×10^3	$590 \times 10^3 (+10\%)$	$490 \times 10^3 (-10\%)$
<i>Mechanical properties</i>			
Resin modulus development model	Model #2, Parameters in [12] Table 6.2	Model #1 ⁽⁶⁾ (see [12] Table B.5) $\alpha_{c1} = 0.608, \alpha_{c2} = 0.750$	
Resin modulus development: Timing (modulus development model #2)	Parameters in [12] Table 6.2	$T_{C1a}^* = -56.7$ K $T_{C2a}^* = -23.0$ K ⁽³⁾	$T_{C1a}^* = -34.7$ K $T_{C2a}^* = -1.0$ K ⁽³⁾
Resin modulus development: Initial modulus (modulus development model #2)	Parameters in [12] Table 6.2	$E^0 = E^{\infty}/10^2$	$E^0 = E^{\infty}/10^4$
Resin cure shrinkage: amount (shrinkage model #1)	Parameters in [12] Table 6.5, ($\alpha_{c2} = 0.67$ actually used)	$V_r^{S\infty} = 0.124 (+25\%)$	$V_r^{S\infty} = 0.074 (-25\%)$
Resin cure shrinkage: timing (shrinkage model #1)	Parameters in Table [12] 6.5	$\alpha_{c1} = 0.05, \alpha_{c2} = 0.77$	$\alpha_{c1} = 0.05, \alpha_{c2} = 0.57$
Composite CTE_3 ($\times 10^{-6}/^{\circ}C$)	28.6	$27.4 + 6 \times 10^{-2} * T^{(4)}$	25.7 (-10%)
J-Frame foot CTE_1 ($\times 10^{-6}/^{\circ}C$)	8.50 (#)	2.9	12.0
Honeycomb moduli (Pa)	$E_{11} = 43.6 \times 10^6, E_{33} = 113 \times 10^6, G_{13} = 16.6 \times 10^6$	$E_{11} = 87.6 \times 10^6, E_{33} = 226 \times 10^6, G_{13} = 33.2 \times 10^6$	$E_{11} = 21.9 \times 10^6, E_{33} = 56.5 \times 10^6, G_{13} = 8.3 \times 10^6$
Honeycomb CTE_1 ($\times 10^{-6}/^{\circ}C$)	10	15	5
Layup accuracy	Perfect	-4° to +4° random angle deviation, both faces	-4° to +4° random angle deviation, both faces
<i>Boundary and initial conditions</i>			
Tool material	Aluminum 'equivalent'	invar 'equivalent'	
Effective heat transfer coefficients (W/m ² K)	Top Side: $4.05 + 2.41 \times 10^{-5} * P$ Bottom Side: $36.6 + 2.00 \times 10^{-4} * P$	Top Side: $6.08 + 3.62 \times 10^{-5} * P (+50\%)$ Bottom Side: $54.9 + 3.00 \times 10^{-4} * P (+50\%)$	Top Side: 4.05 Bottom Side: 36.6 ⁽⁴⁾
P is gage pressure			
Initial degree of cure (-)	$\alpha_0 = 0.05$	$\alpha_0 = 0.15$	$\alpha_0 = 0.01$

Notes:

- (1) Measured variation above Tg
- (2) Room temperature value for nominal case
- (3) Shifts modulus development curve by $\alpha = +/- 0.05$ at a given temperature. Estimated error is based on measurements of modulus development for other materials tested at a range of frequencies
- (4) Based on crude estimates of the variation of specimen CTE_3 with temperature from the original ply measurements (taken from a single chart since no numerical data was available).
- (5) From previous cure kinetics analysis by The Boeing Company
- (6) # - Calibrated value.

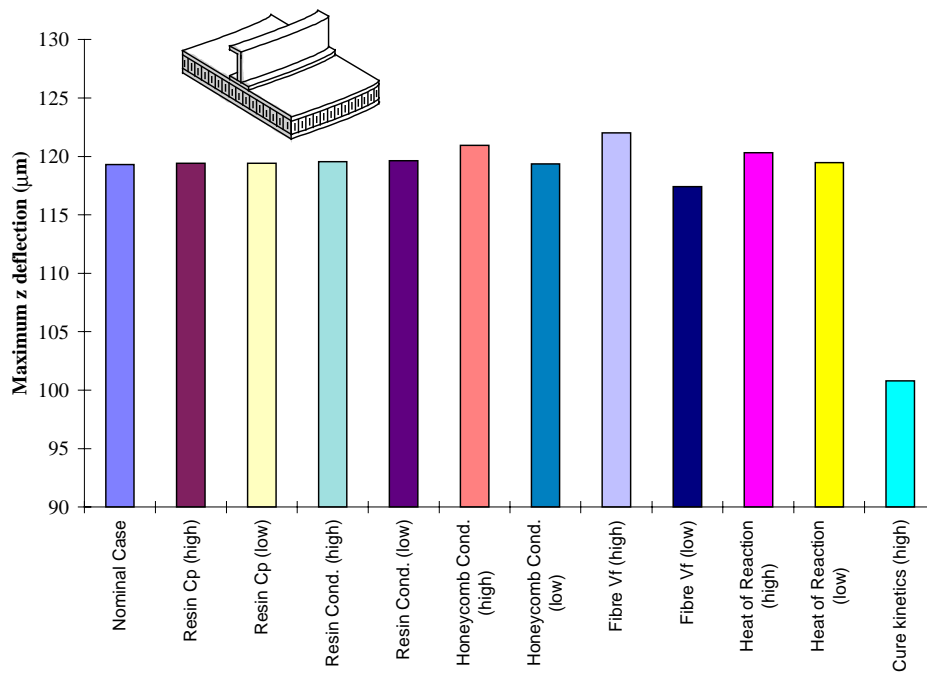


Figure 10. Predicted sensitivity of maximum deformation of stiffened honeycomb structure to variation in thermophysical properties.

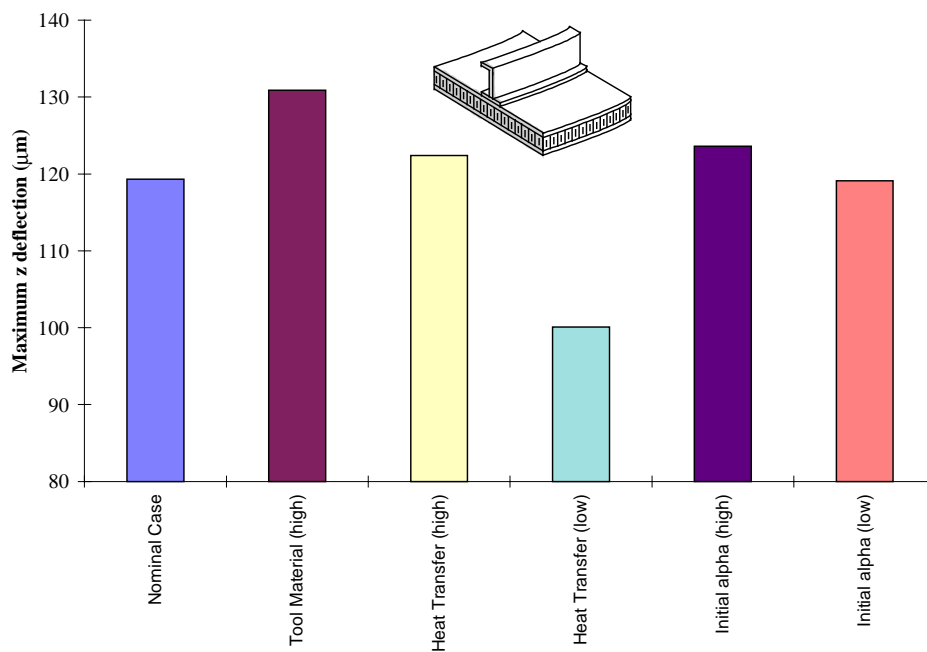


Figure 11. Predicted sensitivity of maximum deformation of stiffened honeycomb structure to variations in boundary and initial conditions.

The predicted sensitivity of structure warpage to mechanical property variations (Figure 12) was significant, with virtually all parameters examined causing at least a 10% shift in model predictions. The most significant was the J-frame foot thermal expansion coefficient, variations in which resulted in changes in model predictions of over 100%. While not insignificant, neither tool material nor initial resin modulus were predominant sources of variation in this analysis.

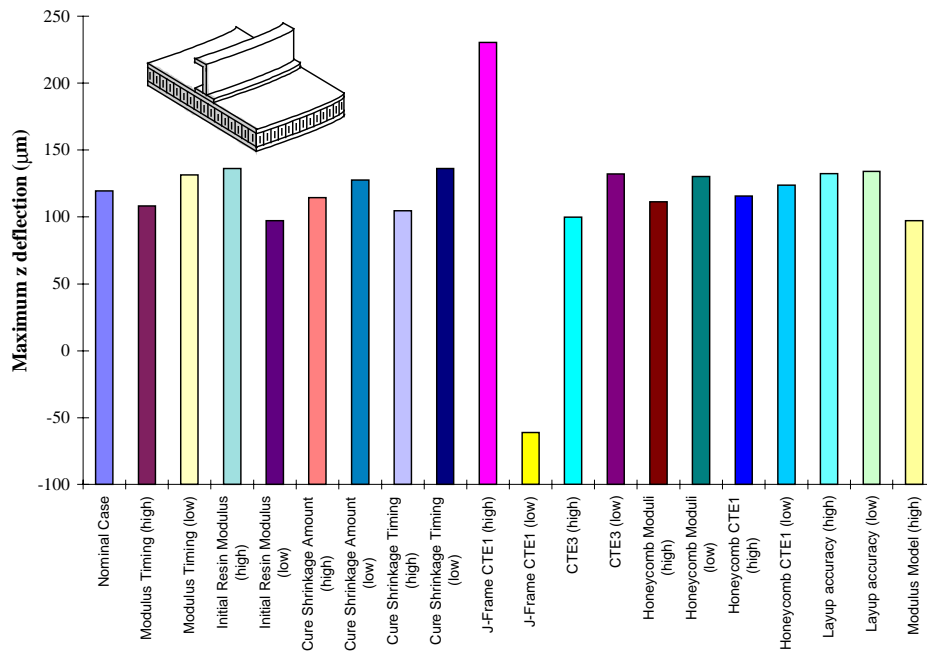


Figure 12. Predicted sensitivity of maximum deformation of stiffened honeycomb structure to variations in mechanical properties.

3. CONCLUSIONS

For the sensitivity analysis performed on the structure presented in this paper, the following conclusions can be drawn:

- Normal variations in composite thermophysical properties had little effect on process model predictions.
- The resin cure kinetics model played an important role, primarily through the effect of cure model predictions on resin hardening and cure shrinkage behaviour rather than its effect on temperature distribution.
- Examination of very local behaviour may be required in some instances in order to get accurate predictions, for example when studying the effects of the J-frame noodle.

4. ACKNOWLEDGMENTS

This paper summarizes work performed over a number of years under funding by the Science Council of British Columbia, the Natural Sciences and Engineering Research Council of Canada, The Boeing Company, The National Aeronautics and Space Administration and Integrated Technologies Inc. We would also like to gratefully acknowledge the significant interaction and support from our colleagues at The Boeing Company and The University of British Columbia.

5. REFERENCES

1. A.C. Loos and G.S. Springer, *J. of Composite Materials*, 17, (2), pp. 135-169 (1983).
2. R. Davé, J.L. Kardos and M.P. Dudukovic, *Proceedings of the American Society for Composites, 1st Technical Conference*, Technomic Publishing, pp. 137-153 (1986).
3. A.R. Mallow, F.R. Muncaster and F.C. Campbell, *Proceedings of the American Society for Composites, Third Technical Conference*, Technomic Publishing, pp. 171-186 (1988).
4. J. Mijovic and J. Wijaya, *SAMPE J.*, 25, (2), 35-39 (1989).
5. T.A. Bogetti and J.W. Gillespie Jr., *J. of Composite Materials*, 26, (5), pp. 626-660 (1992).
6. T.A. Bogetti and J.W. Gillespie Jr., *J. of Composite Materials*, 25, (3), pp. 239-273 (1991).

7. J.M. Kenny, Proceedings of the Third Conference on Computer Aided Design in Composite Materials Technology, pp. 530-544 (1992).
8. S.R. White and H.T. Hahn, J. of Composite Materials, 26, (16), pp. 2402-2422 (1992).
9. H.T. Hahn and N.J. Pagano, J. of Composite Materials, 9, 91-108 (1975).
10. P. Hubert, A. Johnston, R. Vaziri, A. Poursartip, in A. Poursartip and K.N. Street, eds., Proceedings of The 10th International Conference on Composite Materials (ICCM-10), Woodhead Publishing, pp. 149-156, (1995).
11. A. Johnston, P. Hubert, K. Nelson, and A. Poursartip, Proceedings of 38th International SAMPE Technical Conference, pp734-744 (1996).
12. A. Johnston, "An Integrated Model of The Development of Process-Induced Deformation in Autoclave Processing of Composite Structures", Ph.D. Thesis, The University of British Columbia, April 1997